

LAND USE/LAND COVER CHANGES USING LANDSAT IMAGERY IN THE UPPER CITARUM WATERSHED, WEST JAVA, PROVINCE, INDONESIA

Kuswantoro Marko^{1,2}, Dwita Sutjningsih¹, Eko Kusratmoko², Widjojo Adi Prakoso¹

¹ Department of Civil Engineering, Faculty of Engineering, Universitas Indonesia

² Department of Geography, Faculty of Mathematics and Natural Sciences, Universitas Indonesia

email: kuswantoro@sci.ui.ac.id

Received: 10-10-2025; Revised: 09-02-2026; Approved: 10-02-2026

Abstract. Rapid population growth and urban expansion in the Upper Citarum Watershed (UCW) have accelerated Land Use/Land Cover (LULC) changes, particularly the conversion of vegetated and agricultural land into built-up areas. This watershed plays a vital ecological and socio-economic role, supplying water and agricultural resources and supporting three major reservoirs (Saguling, Cirata, and Jatiluhur) that are essential for hydropower generation in Java and Bali. This study analyzes LULC changes over a 30-year period (1990–2020) using multi-temporal Landsat imagery. Landsat Collection-2 Surface Reflectance data (TM, ETM+, and OLI) were processed with cloud and shadow masking and classified using a supervised Maximum Likelihood approach incorporating visible, near-infrared, and shortwave infrared bands. Seven LULC classes were identified: forest, rice field, dry land farming, mixed garden, shrub/grassland, built-up land, and water bodies. The results indicate a substantial increase in built-up land (+16.4% of the watershed area) and a pronounced decrease in rice fields (-11.5%) between 1990 and 2020, largely reflecting conversion from agricultural land. Forest cover declined by 3.2% (approximately 5,705 ha) over the study period. The 2020 classification achieved an overall accuracy of 96% ($\kappa = 0.95$), indicating high reliability, although moderate uncertainty remains among vegetation subclasses. These findings provide an updated long-term perspective on landscape transformation in the UCW and may support watershed management and environmental planning.

Keywords: *LULC, Landsat imagery, remote sensing, GIS, Upper Citarum Watershed*

1 INTRODUCTION

Landuse / landcover (LULC) conversion from natural to built-up areas is a global trend driven by population growth and urbanization, leading to the expansion of cities into rural and higher-elevation areas (Marko et al., 2016; Xie et al., 2024). This shift is motivated by increased demand for housing, industrial development, and economic growth, which often leads to the loss of natural landscapes like forests and agricultural lands. This process has significant consequences for the environment, including increased urban heat islands potential and loss of agricultural productivity (Bikis et al., 2025), can affect the availability of ecosystem services (Keesstra et al., 2018; Hailu et al., 2024; Li et al., 2025), and can increase the potential for flooding and its

losses (Fernandos et al., 2020; Hanifa et al., 2020).

The Citarum watershed is a vital 11,323 km² area in West Java, Indonesia, characterized by the three large reservoirs (Jatiluhur, Cirata, and Saguling) crucial for irrigation and power generation for Java and Madura. The Upper Citarum Watershed (UCW) is densely populated and includes Bandung, the capital of West Java, contributing to the region's high population growth rate and increasing demands for land and water resources (Marko et al., 2021; Mukhoriyah et al., 2023). Over the past three decades, the population of Indonesia, particularly West Java, has grown rapidly, from 32 million in 1990 to 50 million in 2024 (BPS-Statistics of West Java Province, 2024). Likewise, the population of Bandung City and Regency

has increased significantly in the last 30 years, with Bandung City recording 2.41 million people in 2010 and Bandung Regency having a population of around 3.1 million people in 2020, showing consistent growth along with the development of the Bandung metropolitan area (BPS-Statistics of Bandung Regency, 2024).

Studies on changes in LULC in the UCW area over time are very important in efforts to monitor the development of its ecological health. Previous studies in the UCW have employed different sensors, temporal coverage, and classification approaches, including multi-date Landsat analyses by Agaton et al. (2016), Pitaloka et al. (2020), and Yulianto et al. (2019, 2020). While these studies consistently indicate rapid urban expansion and agricultural land loss, variations in class

definitions, reported accuracies, and temporal consistency limit direct inter-decadal comparison. In this study, we adopt a uniform supervised classification workflow applied consistently to Landsat data from 1990 to 2020 to enhance comparability across epochs. Landsat imagery provides the longest continuous Earth observation archive suitable for watershed-scale analysis, balancing spatial resolution and temporal depth. However, this approach is subject to limitations, including spectral confusion among vegetation subclasses and topographic effects in mountainous terrain, which are addressed through the inclusion of shortwave infrared bands, careful training data design, and explicit accuracy assessment.

MATERIALS AND METHODOLOGY

2.1 Study Area

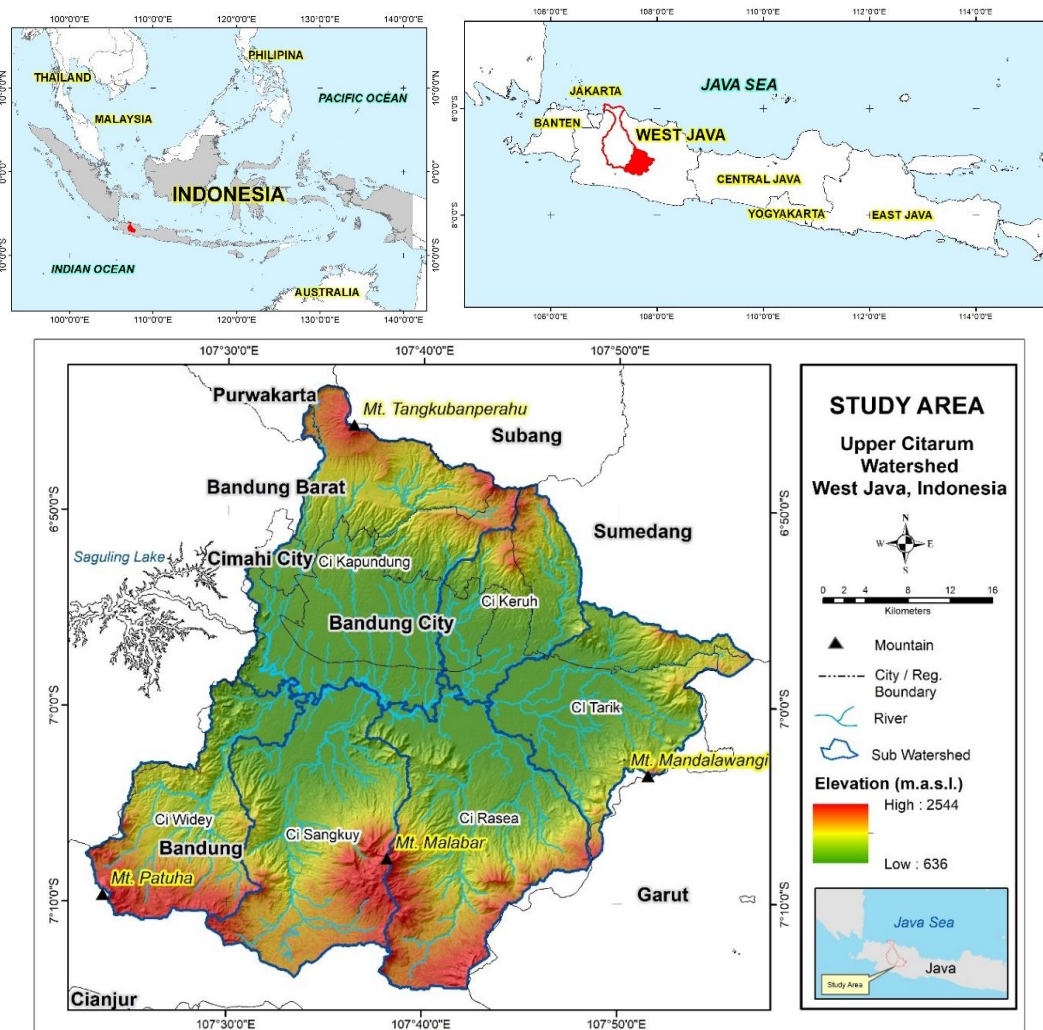


Figure 2-1: Study area of the Upper Citarum Watershed (UCW), West Java, Indonesia (UCW boundary overlaid on Landsat imagery; data source: BIG and Landsat)

This Research was conducted at the Upper Citarum Watershed (UCW) at coordinates 6°43'-7°15'S and 107°30'-108°E. Administratively, this study area covers Bandung Regency and City, Cimahi City, West Bandung Regency, Subang, Garut, and Sumedang Regencies. The whole of Citarum watershed is the widest and longest watershed in West Java Province where the city of Bandung is in UCW which has caused rapid population growth and activities every year. In 2020, the total population of the UCW is around nine million people out of a total of 49 million people or almost 20% of the total population in West Java Province (BPS-Statistics of West Java Province, 2020).

The UCW is divided into six sub watersheds i.e. Cikapundung, Ciwidey. Cikeruh, Cisangkuy, Citarik, and Cirasea (Khairunnisa et al., 2020; Hanifa et al., 2020; Marko et al., 2021). Geomorphologically, this research area is dominated by flat relief with slopes < 7% which covers about 47% of the total area. The altitude of the area ranges from 636 to 2,544 meters above sea level. The central part of this watershed has a broad flat relief known as the plateau. This watershed is surrounded by mountain

ranges such as Tangkuban Perahu in the north, Patuha-Malabar in the south, and Mandalawangi in the east (See Figure 2-1).

2.2 Landsat Data and Pre-processing

LULC mapping was based on Landsat Collection-2 Surface Reflectance products from Landsat-5 TM, Landsat-7 ETM+, and Landsat-8 OLI for the reference years 1990, 2000, 2010, and 2020 (See Table 2-1). For each year, cloud-minimized scenes from path/row 121/65 and 122/65 acquired during the dry season were selected and mosaicked to cover the entire UCW. Cloud and cloud-shadow masking were performed using the CFMask algorithm prior to analysis.

All images were radiometrically and geometrically corrected and converted to surface reflectance. Spectral inputs included TM bands 1-5 and 7, and OLI bands 2-7, incorporating shortwave infrared bands to improve discrimination among vegetation, soil, moisture conditions, and built-up areas. To reduce topographic illumination effects in mountainous regions, a DEM-based terrain normalization was applied prior to classification.

Table 2-1: Characteristics of the satellite data used in the study area

Landsat	Sensor	Spatial resolution (m)	Wave length range (micro-m)	Selected bands	Path/row	Acquisition date
5	TM	30	0.45-0.90	1-5,7	122/065	09/07/1990
5	TM	30	0.45-0.90	1-5,7	121/065	04/09/1990
5	TM	30	0.45-0.90	1-5,7	122/065	05/08/2000
5	TM	30	0.45-0.90	1-5,7	121/065	11/06/2000
5	TM	30	0.45-0.90	1-5,7	122/065	01/08/2010
5	TM	30	0.45-0.90	1-5,7	121/065	09/07/2010
8	OLI	30	0.45-0.885	2-7	122/065	27/07/2020
8	OLI	30	0.45-0.885	2-7	121/065	20/08/2020

The type of LULC determined consists of seven types i.e. forest, bush-grass, mixed gardens, dry land farming, rice fields, built-up land, and water bodies (See Table 2-2). The identification of the type of LULC is based on color, shape, size, pattern, texture, location, and object appearance

associations. Sample Area is needed as the basis for identifying objects in the image and the Maximum Likelihood method which has the principle that every pixel in each class in space will be normally distributed and in making grouping decisions using bias theory is applied.

Table 2-2: Land use/land cover classification scheme

ID	LULC Type	Description
1	Water Body	Reservoir/lakes
2	Forest	Primary and secondary forest
3	Bush-Grass	Reeds, grass, bushes
4	Mixed Garden	Trees interspersed with reeds and grass
5	Dry Land Farming	Moor, field
6	Rice Field	Irrigated and rainfed rice fields
7	Built-up land	Residential, industrial area, tourist area

2.3 Training Data and Supervised Classification

Training data were generated independently for each reference year using a stratified approach, ensuring that all LULC classes were adequately represented. Training polygons were digitized through visual interpretation of Landsat composites supported by a 1:25,000 digital topographic map from the Geospatial Information Agency (BIG, 2017) and epoch-proximate high-resolution imagery available in Google Earth. Ambiguous sites were reviewed by two interpreters, and only consensus samples were retained to minimize labeling bias. A minimum of 30 training polygons per class per year were used. Supervised classification was performed using the Maximum Likelihood Classifier implemented in ENVI and ArcGIS, assuming multivariate normal distributions and equal prior probabilities. This classifier was selected for its robustness and long-standing application in multi-temporal Landsat-based LULC studies.

2.4 Accuracy Assessment

An accuracy assessment was conducted using stratified random sampling with reference samples distributed across all mapped classes. Validation data for 2020 were derived from very-high-resolution Google Earth imagery supported by field-verified points. For earlier years, historical high-resolution imagery and archival spatial references were used where available to reduce temporal labeling bias. Confusion matrices were used to derive Overall Accuracy (OA), Producer's Accuracy (PA), and User's Accuracy (UA). Cohen's Kappa (κ) coefficient was calculated as supplementary information. Accuracy results are presented prior to

LULC change analysis to establish classification reliability.”

The method that is widely used is the Cohen's Kappa (κ) coefficient accuracy test as carried out by Marko et al. (2016), Rwanga & Ndambuki (2017), Pande et al. (2021), and Islami et al. (2022). Accuracy testing is carried out by creating a contingency or error matrix or also known as a confusion matrix. The accuracy test procedure is as described by Islami et al. (2022) as follows:

- (1) Calculating User Accuracy: Number of correctly classified pixels in each category divided by total number of reference pixels in that category (the row total), then multiplied by 100.
- (2) Calculating Producer Accuracy: Number of correctly classified pixels in each category divided by total number of reference pixels in that category (the column total), then multiplied by 100.
- (3) Calculating Overall Accuracy: Total number of correctly classified pixels (diagonal) divided by total number of reference pixels, then multiplied by 100.
- (4) Calculating Cohen's Kappa (κ) coefficient:

$$\kappa = \frac{(N \times D) - Q}{N^2 - Q}$$

where :

N = Total number of pixels calculated

D = Total number of the correct pixels

Q = Multiplication between each total pixels per class in user accuracy and producer accuracy

Overall Accuracy, Producer's Accuracy, User's Accuracy, and Cohen's Kappa were computed from confusion matrices following standard remote sensing accuracy assessment procedures.

3. RESULT AND DISCUSSION

3.1 LULC Accuracy Test

The image accuracy test is conducted for classification or processing errors, so that the percentage of accuracy of the classification results can be known. Accuracy test is done by creating contingency or commonly called error matrix or confusion matrix (Nawangwulan, 2013). This accuracy test is done by comparing the LULC classification data of Landsat imagery in 2020 with high resolution imagery sourced from Google Earth in 2020 which had previously been checked in the field on LULC

The following is the distribution of the locations tested for accuracy as shown in Figure 3-1 the following.

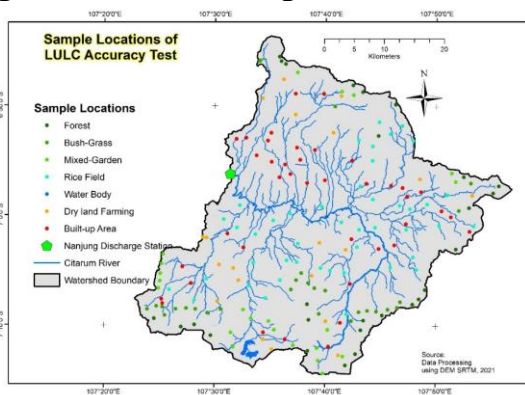


Figure 3-1: Distribution of sample locations of LULC accuracy test

The results of the accuracy test as follow:

1) Tabel of Confusion Matrix

Confusion matrix table (See Table 3-1) in this accuracy test, it contains field data and LULC classification results, then produces Producer Accuracy and User Accuracy values.

2) Calculation Results of User Accuracy

The value of user accuracy is to show the accuracy of the classification of all objects that have been identified. The calculation results as follows:

- a. *User accuracy* water body : $19/19 \times 100 = 100\%$
- b. *User accuracy* forest : $26/27 \times 100 = 96.3\%$
- c. *User accuracy* mixed garden : $20/23 \times 100 = 87\%$
- d. *User accuracy* bush grass : $25/27 \times 100 = 92.6\%$
- e. *User accuracy* built-up land : $40/40 \times 100 = 100\%$
- f. *User accuracy* rice field : $44/44 \times 100 = 100\%$

- g. *User accuracy* dry land farming : $18/20 \times 100 = 90\%$

3) Calculation Results of Producer Accuracy

The value of producer accuracy is to show the correctness of the classification in the field. The calculation results as follows:

- a. *Producer accuracy* water body : $19/19 \times 100 = 100\%$
- b. *Producer accuracy* forest : $26/30 \times 100 = 86.7\%$
- c. *Producer accuracy* mixed garden: $20/20 \times 100 = 100\%$
- d. *Producer accuracy* bush grass : $25/25 \times 100 = 100\%$
- e. *Producer accuracy* built-up land : $40/40 \times 100 = 100\%$
- f. *Producer accuracy* rice field : $44/44 \times 100 = 100\%$
- g. *Producer accuracy* dry land farming : $18/22 \times 100 = 81.8\%$

4) Calculation Results of Overall accuracy

The overall accuracy value is the overall accuracy value. The calculation results of the overall accuracy as follows: $192/200 = 0,96$ or 96% .

5) Determination Results of Cohen's Kappa (κ) coefficient

The calculation of Cohen's Kappa (κ) coefficient considers the value of producer accuracy and user accuracy. The Cohen's Kappa (κ) coefficient calculation formula is as follows:

$$\kappa = \frac{(N \times D) - Q}{N^2 - Q}$$

$$\kappa = \frac{(N \times D) - Q}{N^2 - Q}$$

where :

N = Total of pixel : 200

D = Total of the true pixel : $19+26+20+25+40+44+18 = 192$

Q = Multiplication between each total pixel per class in user accuracy and producer accuracy: $(19 \times 19) + (27 \times 30) + (23 \times 20) + (27 \times 25) + (40 \times 40) + (44 \times 44) + (20 \times 22) = 6282$

Calculation of Cohen's Kappa (κ) coefficient in this study is:

$$\kappa = \frac{(200 \times 192) - 6282}{(200)^2 - 6282}$$

$$\kappa = \frac{(200)^2 - 6282}{(200)^2 - 6282} = 0,95$$

Based on the result of Cohen's Kappa (κ) coefficient, the accuracy of the LULC

classification using Landsat imagery is in category almost perfect agreement.

Tabel 3-1: Tabel of Confusion Matrix

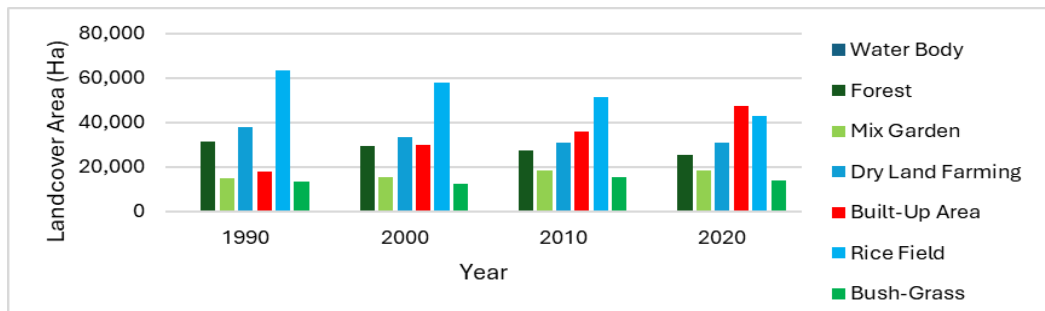
LULC Classification	Observation Data								User Accuracy
	WB	FR	MG	BG	BL	RF	DLF	Total	
Water Body (WB)	19	-	-	-	-	-	-	19	100.0
Forest (FR)	-	26	-	-	-	-	1	27	96.3
Mixed-Garden (MG)	-	-	20	-	-	-	3	23	87.0
Bush-Grass (BG)	-	2	-	25	-	-	-	27	92.6
Built-up Land (BL)	-	-	-	-	40	-	-	40	100.0
Rice Field (RF)	-	-	-	-	-	44	-	44	100.0
Dry Land Farming (DLF)	-	2	-	-	-	-	18	20	90.0
Total	19	30	20	25	40	44	22	200	
Producer Accuracy	100	86.7	100	100	100	100	81.8		

(Source: Data processing, 2020)

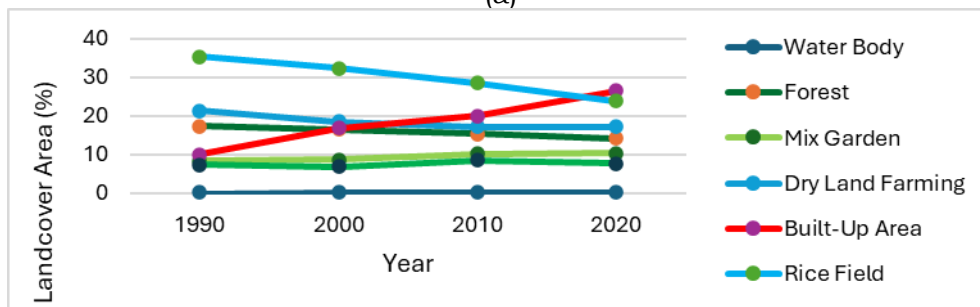
3.2 LULC Classification and Changes

The 2020 LULC classification achieved an overall accuracy of 96% with a Cohen’s Kappa coefficient of 0.95, indicating high overall reliability. The lowest producer’s accuracy was observed for dry land farming (81.8%), suggesting moderate confusion with mixed gardens and shrub/grassland classes. These uncertainties are considered in interpreting subsequent change analyses. Based on the LULC classification using supervised method, the LULC classification in each period can be explained. In 1990, rice fields had the dominant area (63,304 ha or 35.4%)

followed by dry land agriculture (38,087 ha or 21.3%) and forests (31,163 ha or 17.4%). In 2000, the area of built-up land increased to almost the same area as dryland agriculture. In 2010, it was clearly seen that rice fields and built-up land dominated, although rice fields were decreasing, followed by dry land farming and forest. In 2020, the most dominant built-up land (47,417 ha or 26.5%) followed by rice fields (42,792 ha or 23.9%), dry land farming (17.2%), forests (14.2%), mixed gardens (10.3%), bush-grass (7.6%), and water bodies (0.2%) as shown in Figure 3-2.



(a)



(b)

Figure 3-2: The changes of landcover area in each ten year from 1990 to 2020

Changes in LULC in each period can be described as follows. In the period 1990 to 2000, the area of built-up land increased by 6.7%, while rice fields and dry land decreased by 3% and 2.7%, respectively. In the period 2000 to 2010, built-up land continued to increase by 3.7%, while rice fields decreased by 3.7%. In the 2010 to 2020 period, built-up land increased by 6.5%, while rice fields decreased by 4.7%.

When viewed over the last 30 years, the area of built-up LULC increased rapidly by 16.4% of the total watershed area or about 29,350 ha, which was accompanied by a decrease in the area of rice fields by 11.5% and dry land agriculture by 4.1%. The type of forest LULC decreased which was not so significant, namely 3.2% or 5,705 ha when compared to the decrease in the area of rice fields (See Table 3-2).

Table 3-2: Landcover changes for each ten year and the last 30 year in the Upper Citarum Watershed

Landcover Type	Δ 1990 - 2000		Δ 2000 - 2010		Δ 2010 - 2020		Δ 1990 -2020	
	Ha	%	ha	%	Ha	%	ha	%
Water Body	+14	0.0	+11	0.0	+114	+0.1	+139	+0.1
Forest	-1,549	-0.9	-2,262	-1.3	-1,894	-1.1	-5,679	-3.2
Mix Garden	+693	+0.4	+2,816	+1.6	+145	+0.1	+3,654	+2.0
Dry Land Farming	-4,848	-2.7	-2,431	-1.4	-67	0.0	-7,346	-4.1
Built-up land	+12,017	+6.7	+5,692	+3.2	+11,641	+6.5	+29,350	+16.4
Rice Field	-5,396	-3.0	-6,697	-3.7	-8,419	-4.7	-20,512	-11.5
Bush-Grass	-931	-0.5	+2,871	+1.6	-1,520	-0.8	+420	+0.2

In detail, LULC changes in the UCW over the last 30 years can be shown in Tables 3-3 and 3-4 below. Based on the table, the built-up LULC has a percentage value of 99.2% to remain as built-up land. This shows that the built-up land has always experienced an expansion of the area originating from rice fields (17,802 ha), dryland agriculture (8,887 ha), mixed gardens (1,839 ha) and forests (831 ha).

The forest LULC has a fixed percentage value as forest land of 77.9%. As much as

22.1% of the forest land has been changed to other LULC, most of which are mixed gardens (4,440 ha), followed by dryland agriculture, built up land, and bush-grass. Likewise, rice fields have decreased by 20,512 ha in the past 30 years. Most of the conversion of paddy fields to built-up land (17,802 ha), followed by dryland agriculture, mixed gardens, bush-grass, and a small portion to forest (See Table 3-4).

Table 3-3: Matrix of LULC change in the last 30 years (1990-2020) in the UCW (percent units)

Landcover Change Matrix		Landcover 2020							Grand Total
		Water body	Forest	Mix Garden	Dry Land Farming	Built-Up Land	Rice Field	Bush-Grass	
Landcover 1990	Water body	77.5	0.2	2.0	0.9	16.9	0.0	2.5	100
	Forest	0.0	77.9	14.3	3.1	2.7	0.0	2.0	100
	Mixed Garden	0.1	1.6	79.2	5.5	12.4	0.0	1.2	100
	Dry Land Farming	0.0	1.4	2.4	71.6	23.3	0.0	1.2	100
	Built-Up Land	0.0	0.0	0.1	0.6	99.2	0.0	0.1	100
	Rice Field	0.2	0.5	1.0	2.0	28.1	67.6	0.6	100
	Bush-Grass	0.0	0.7	5.7	2.2	0.7	0.0	90.8	100
	Grand Total	0.2	14.2	10.3	17.2	26.5	23.9	7.6	100

Tabel 3-4: Matrix of LULC change in the last 30 years (1990-2020) in the UCW (hectare units)

Landcover Change Matrix		Landcover 2020							
		Water body	Forest	Mix Garden	Dry Land Farming	Built-Up Land	Rice Field	Bush-Grass	Grand Total
Landcover 1990	Water body	164	0.5	4.2	1.8	36	0.0	5.2	212
	Forest	12	24,265	4,440	966	831	11	609	31,133
	Mixed Garden	16	243	11,751	822	1,839	0.0	173	14,844
	Dry Land Farming	16	549	900	27,282	8,887	0.0	453	38,087
	Built-Up Land	5.7	5.9	10	107	17,927	0.0	11	18,066
	Rice Field	112	297	642	1,273	17,802	42,782	395	63,303
	Bush-Grass	0.6	94	750	289	92	0.0	12,034	13,260
	Grand Total	326	25,454	18,498	30,741	47,415	42,792	13,680	178,905

Spatially, LULC changes can be reviewed based on the sub-watersheds consisting of the Ci Kapundung, Ci Keruh, and Ci Tarik sub-watersheds in the northern part, and the Ci Rasea, Ci Sangkuy, and Ci Widey sub-watersheds in the southern part of the study area. Forest land is spread over hilly areas in each sub-watershed. In 1990 the Ci Sangkuy Sub-watershed has the largest forest area, followed by Ci Widey and Ci Rasea, while the Ci Keruh Sub-watershed has the narrowest forest area. The forest area in each period decreases. Meanwhile,

mixed gardens and bush-grass experienced fluctuations in land area in each sub-watershed. Built-up land has increased in each sub-watershed, where the Ci Kapundung sub-watershed is the area that has the largest built-up land and in 2020 the land area has increased twice from 1990. The rice fields also experienced a decrease in area, where in 1990 the sub-Ci Kapundung watershed has the largest rice field area, which then in 2020 the area of the land was significantly reduced (See Figure 3-3).

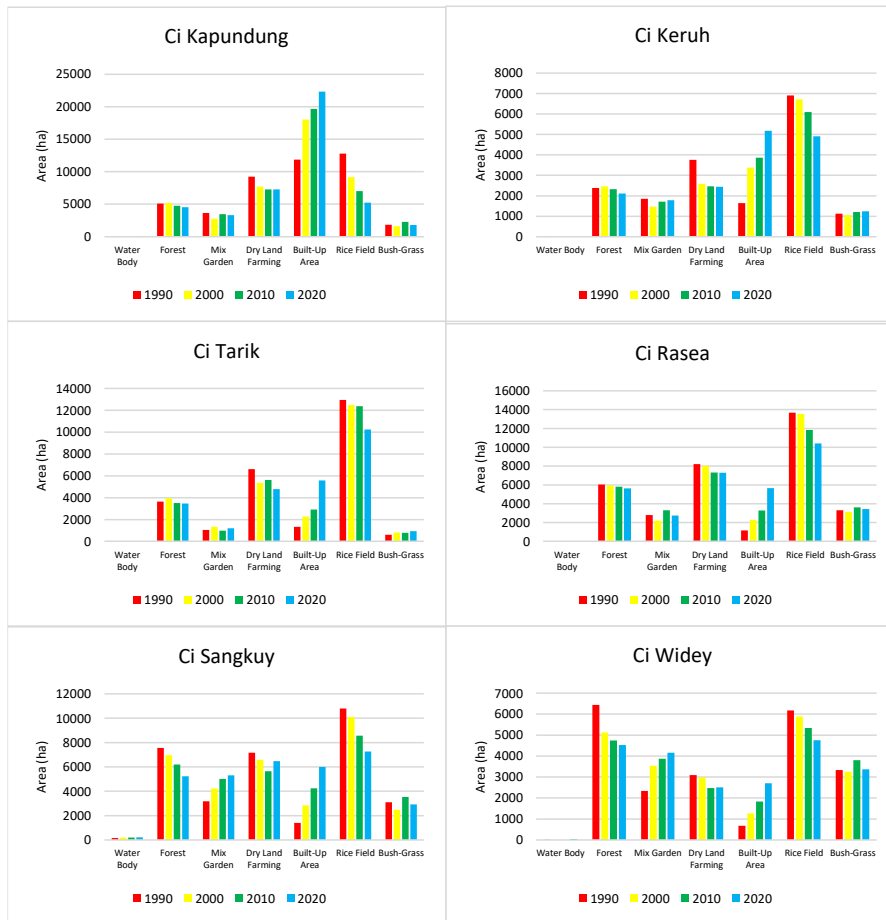


Figure 3-3: Landcover changes in each Sub Watershed

Figure 3-4 shows how the built-up land developed from 1990 to 2020. In 1990, the built-up land was centered around the city of Bandung, namely in the middle-west part, which then in 2000 expanded to various directions which were originally rice fields. In 2010 and 2020, the built-up land is expanding to the south, namely in the Ci Sangkuy, Ci Rasea, and Ci Tarik sub-watersheds. It is clear that the rice fields are narrowing and changing. Meanwhile, forest land has decreased in area, especially around the Malabar

mountains in the Ci Sangkuy sub-watershed which has been converted into bush-grass, mixed gardens, and built-up land. In the area there is a reservoir that has a function as a tourist destination. This spatial pattern suggests a possible association with tourism-related and infrastructure development; however, this interpretation should be regarded as a hypothesis that requires confirmation using independent socio-economic or land-permit datasets.

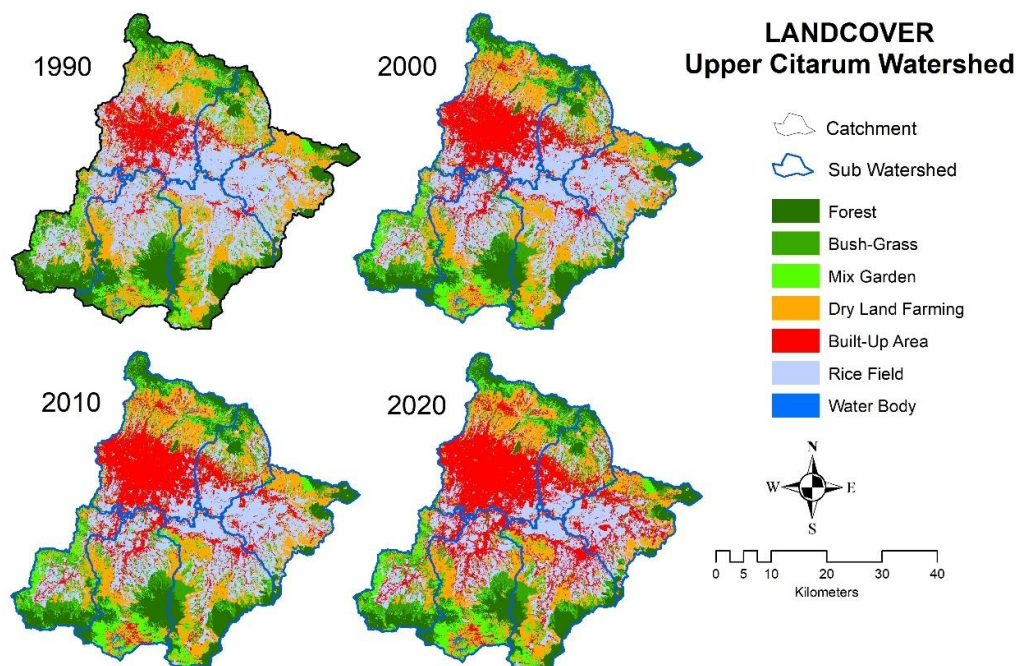


Figure 3-4: The changes of landcover area in each ten year from 1990 to 2020

4 CONCLUSIONS

This study analyzed LULC changes in the Upper Citarum Watershed over a 30-year period (1990–2020) using multi-temporal Landsat imagery and a consistent supervised classification framework. The results show a substantial increase in built-up land (+16.4%) accompanied by marked declines in rice fields (-11.5%) and dry land farming (-4.1%). Forest cover also decreased by 3.2% (approximately 5,705 ha), indicating gradual but persistent loss of natural vegetation.

The 2020 classification achieved high overall accuracy (>95%), indicating strong reliability of the LULC maps, although moderate uncertainty remains among

vegetation subclasses. These findings highlight the continuing transformation of the UCW landscape and underscore the importance of integrating long-term remote sensing analysis into watershed management and spatial planning strategies.

ACKNOWLEDGMENT

The authors would like to thank the Directorate of Research and Community Engagement (DPRM) University Indonesia for the research funding program Publikasi Terindeks Internasional (PUTI) Doktor in 2020 No. NKB-3359/UN2.RST/HKP.05.00/2020.

REFERENCES

- AGATON, M., SETIAWAN, Y., & EFFENDI, H. (2016). LAND USE/LULC CHANGE DETECTION IN AN URBAN WATERSHED: A CASE STUDY OF UPPER CITARUM WATERSHED, WEST JAVA PROVINCE, INDONESIA. *PROCEDIA ENVIRONMENTAL SCIENCES*, 33, 654–660. [HTTPS://DOI.ORG/HTTPS://DOI.ORG/10.1016/J.PROENV.2016.03.120](https://doi.org/https://doi.org/10.1016/j.proenv.2016.03.120)
- BPS-STATISTICS OF JAWA BARAT PROVINCE. (2020). JAWA BARAT PROVINCE IN FIGURES 2020. AVAILABLE AT: [HTTPS://JABARPROV.GO.ID/ASSETS/DATA/MENU/PROVINSI%20JAWA%20BARAT%20DALAM%20ANGKA%202020.PDF](https://jabarprov.go.id/assets/data/menu/provinsi%20JAWA%20BARAT%20DALAM%20ANGKA%202020.pdf)
- BPS-STATISTICS OF BANDUNG REGENCY. (2024). [HTTPS://BANDUNGKAB.BPS.GO.ID/ID/STATISTICS-TABLE/1/MTk2IzE=/JUMLAH-PENDUDUK-MENURUT-KABUPATEN-KOTA-DI-PROVINSI-JAWA-BARAT--RIBU--2010.HTML](https://bandungkab.bps.go.id/id/statistics-table/1/MTk2IzE=/JUMLAH-PENDUDUK-MENURUT-KABUPATEN-KOTA-DI-PROVINSI-JAWA-BARAT--RIBU--2010.HTML)
- BIKIS, A., ENGDAW, M., PANDEY, D. *ET AL.* THE IMPACT OF URBANIZATION ON LAND USE LAND COVER CHANGE USING GEOGRAPHIC INFORMATION SYSTEM AND REMOTE SENSING: A CASE OF MIZAN AMAN CITY SOUTHWEST ETHIOPIA. *SCI REP* **15**, 12014 (2025). [HTTPS://DOI.ORG/10.1038/S41598-025-94189-6](https://doi.org/10.1038/s41598-025-94189-6)
- FERNANDOS, TAMBUNAN, M. P., & MARKO, K. (2020). LOSS LEVELS REGARDING FLOOD AFFECTED AREAS IN THE UPPER CITARUM WATERSHED. *IOP CONFERENCE SERIES: EARTH AND ENVIRONMENTAL SCIENCE*, 561(1), 12027. [HTTPS://DOI.ORG/10.1088/1755-1315/561/1/012027](https://doi.org/10.1088/1755-1315/561/1/012027)
- PITALOKA, E.F., KARUNIASA, M., & MOERSIDIK, S.S. (2020). TIME SERIES OF FOREST LULC CHANGE IN THE UPPER CITARUM WATERSHED, WEST JAVA PROVINCE, INDONESIA. *E3S WEB CONF.*, 211. [HTTPS://DOI.ORG/10.1051/E3SCONF/202021104001](https://doi.org/10.1051/e3sconf/202021104001)
- HAILU T, ASSEFA E & ZELEKE T (2024) URBAN EXPANSION INDUCED LAND USE CHANGES AND ITS EFFECT ON ECOSYSTEM SERVICES IN ADDIS ABABA, ETHIOPIA. *FRONT. ENVIRON. SCI.* 12:1454556. DOI: 10.3389/FENV.2024.1454556
- HANIFA, S., TAMBUNAN, M. P., & MARKO, K. (2020). RAINFALL DISTRIBUTION IN RELATION TO FLOODING IN UPPER CITARUM WATERSHED, INDONESIA. *IOP CONFERENCE SERIES: EARTH AND ENVIRONMENTAL SCIENCE*, 500(1), 12088. [HTTPS://DOI.ORG/10.1088/1755-1315/500/1/012088](https://doi.org/10.1088/1755-1315/500/1/012088)
- ISLAMI, F. A., TARIGAN, S. D., WAHJUNIE, E. D., & DASANTO, B. D. (2022). ACCURACY ASSESSMENT OF LAND USE CHANGE ANALYSIS USING GOOGLE EARTH IN SADAR WATERSHED MOJOKERTO REGENCY. *IOP CONFERENCE SERIES: EARTH AND ENVIRONMENTAL SCIENCE*, 950(1), 12091. [HTTPS://DOI.ORG/10.1088/1755-1315/950/1/012091](https://doi.org/10.1088/1755-1315/950/1/012091)
- KEESSTRA, S., NUNES, J., NOVARA, A., FINGER, D., AVELAR, D., KALANTARI, Z., & CERDA, A. (2018). THE SUPERIOR EFFECT OF NATURE BASED SOLUTIONS IN LAND MANAGEMENT FOR ENHANCING ECOSYSTEM SERVICES. IN SCIENCE OF THE TOTAL ENVIRONMENT. [HTTPS://DOI.ORG/10.1016/J.SCITOTENV.2017.08.077](https://doi.org/10.1016/j.scitotenv.2017.08.077)
- LI, M., CAO, Y., DAI, J., SONG, J., & LIANG, M. (2025). A COMPREHENSIVE REVIEW OF URBAN EXPANSION AND ITS DRIVING FACTORS. *LAND*, 14(8), 1534. [HTTPS://DOI.ORG/10.3390/LAND14081534](https://doi.org/10.3390/land14081534)
- LIAO, H., SARVER, E., & KROMETIS, L. A. H. (2018). INTERACTIVE EFFECTS OF WATER QUALITY, PHYSICAL HABITAT, AND WATERSHED ANTHROPOGENIC ACTIVITIES ON STREAM ECOSYSTEM HEALTH. *WATER RESEARCH*. [HTTPS://DOI.ORG/10.1016/J.WATRES.2017.11.065](https://doi.org/10.1016/j.watres.2017.11.065)
- MARKO, K., ZULKARNAIN, F., & KUSRATMOKO, E. (2016). COUPLING OF MARKOV CHAINS AND CELLULAR AUTOMATA SPATIAL MODELS TO PREDICT LAND COVER CHANGES (CASE STUDY: UPPER CI LEUNGI CATCHMENT AREA). *IOP CONFERENCE SERIES: EARTH AND ENVIRONMENTAL SCIENCE*, 47(1), 12032. [HTTPS://DOI.ORG/10.1088/1755-1315/47/1/012032](https://doi.org/10.1088/1755-1315/47/1/012032)
- MARKO, K., SUTJININGSIH, D., & KUSRATMOKO, E. (2021). WATERSHED HEALTH CHANGES BASED ON VEGETATED LAND COVER IN THE UPPER CITARUM WATERSHED, WEST JAVA, PROVINCE, INDONESIA. *IOP CONFERENCE SERIES: EARTH AND ENVIRONMENTAL SCIENCE*, 940(1), 12045. [HTTPS://DOI.ORG/10.1088/1755-1315/940/1/012045](https://doi.org/10.1088/1755-1315/940/1/012045)
- MUKHORAYAH, M., ARIFIN, S., KUSHARDONO, D., ARDHA, M., & YULIANTO, F. (2023). ANALYSIS OF LAND USE AND SPATIAL PLANNING IN THE UPSTREAM CITARUM WATERSHED OF WEST JAVA BASED ON REMOTE SENSING DATA. *JOURNAL OF DEGRADED AND MINING LANDS MANAGEMENT*, 10(3), 4315–4324. [HTTPS://DOI.ORG/10.15243/JDMLM.2023.103.4315](https://doi.org/10.15243/jdmlm.2023.103.4315)
- PANDE, C. B., MOHARIR, K. N., & KHADRI, S. F. R. (2021). ASSESSMENT OF LAND-USE AND LAND-COVER CHANGES IN PANGARI WATERSHED AREA (MS), INDIA, BASED ON THE REMOTE SENSING AND GIS TECHNIQUES. *APPLIED WATER SCIENCE*, 11(6), 96. [HTTPS://DOI.ORG/10.1007/S13201-021-01425-1](https://doi.org/10.1007/s13201-021-01425-1)
- RWANGA, S. & NDAMBUKI, J. (2017) ACCURACY ASSESSMENT OF LAND USE/LAND COVER CLASSIFICATION USING REMOTE SENSING AND GIS. *INTERNATIONAL JOURNAL OF GEOSCIENCES*, **8**, 611-622. DOI: 10.4236/IJG.2017.84033.
- XIE, H., SUN, Q., & SONG, W. (2024). EXPLORING THE ECOLOGICAL EFFECTS OF RURAL LAND USE CHANGES: A BIBLIOMETRIC OVERVIEW. *LAND*, 13(3), 303. [HTTPS://DOI.ORG/10.3390/LAND13030303](https://doi.org/10.3390/land13030303)
- YULIANTO, F., MAULANA, T., & KHOMARUDIN, M. R. (2019). ANALYSIS OF THE DYNAMICS OF LAND USE CHANGE AND ITS PREDICTION BASED ON THE INTEGRATION OF REMOTELY SENSED DATA AND CA-MARKOV MODEL, IN THE UPSTREAM CITARUM WATERSHED, WEST JAVA, INDONESIA. *INTERNATIONAL JOURNAL OF DIGITAL EARTH*, 12(10), 1151–1176. [HTTPS://DOI.ORG/10.1080/17538947.2018.1497098](https://doi.org/10.1080/17538947.2018.1497098)
- YULIANTO, F., SUWARSONO, S., NUGROHO, U. C., NUGROHO, N. P., SUNARMODO, W., & KHOMARUDIN, M. R. (2020). SPATIAL-TEMPORAL DYNAMICS LAND USE/LULC CHANGE AND FLOOD HAZARD MAPPING IN THE UPSTREAM CITARUM WATERSHED, WEST JAVA, INDONESIA. *QUAESTIONES GEOGRAPHICAE*, 39(1), 125–146. [HTTPS://DOI.ORG/10.2478/QUAGEO-2020-0010](https://doi.org/10.2478/QUAGEO-2020-0010)